

An Atomic Oxygen Beam System for the Investigation of Mass Spectrometer Response in the Upper Atmosphere*

HASSO B. NIEMANN†

Department of Electrical Engineering, Space Physics Research Laboratory, The University of Michigan, Ann Arbor, Michigan 48105

(Received 2 March 1972; and in final form, 5 May 1972)

An atomic oxygen beam system has been designed and tested for the laboratory evaluation of mass spectrometers used in upper atmospheric measurements. The atomic oxygen is generated by thermal dissociation of molecular oxygen on the surface of a tungsten filament heated to 2800 K. A symmetrical bidirectional beam is produced to permit simultaneous monitoring of the particle flux in the beam while target experiments are being conducted. Flux levels of 5×10^{14} particles $\text{cm}^{-2} \text{sec}^{-1}$ over a cross-sectional area of 1 cm^2 have been produced with a relative atomic oxygen concentration of 70%. At flux levels below 10^{13} particles $\text{cm}^{-2} \text{sec}^{-1}$, relative atomic oxygen concentrations of more than 90% were obtained. The oxygen beam is of high purity and free from chemically active contaminants. Strong chemical and low temperature pumping are used to reduce background gas contributions to less than 1%. Measurements of the relative atomic concentration in the beam were made with a quadrupole spectrometer using an open flowthrough ion source. The absolute flux of molecular oxygen was determined with the aid of an enclosed omegatron mass spectrometer. The combined use of both instruments permitted a determination of the magnitude of the atomic oxygen flux in the beam.

INTRODUCTION

The proper interpretation of data obtained from rocket or satellite borne mass spectrometer measurements of atomic oxygen presents serious difficulties. Because of its high chemical activity, atomic oxygen reacts strongly with the instrument chamber walls, and many of the oxygen atoms are permanently absorbed on the surface, or recombined to molecular oxygen. As a result of these losses, the measured concentrations of atoms are lower than the actual atmospheric density.

Improvement can be obtained by using quasiopen ion sources; in this case fewer surface collisions per particle occur, but one must deal with more complex gas dynamic conditions.

To simulate the conditions encountered during a rocket or satellite flight accurately, a high velocity and low density atomic and molecular beam system is needed. The required kinetic energy ranges from approximately 0.25 eV for rocket experiments to 8.0 eV for satellite experiments. Particle beams of this energy are difficult to obtain with any gas, and the problem is further complicated with atomic oxygen because its chemical activity makes it difficult to produce and to maintain.

In this paper, an atomic oxygen beam system is described with which it is possible to generate a pure oxygen beam of high relative atomic concentration. Oxygen atoms are produced by thermal dissociation of oxygen molecules on a hot tungsten filament. The emitted oxygen atoms and molecules are collimated to form a particle beam. Relative atomic concentrations of more than 70% are obtained over a flux range which simulates atmospheric conditions from about 150 to 350 km. The average thermal velocity of the emitted oxygen atoms is close to velocities expected in rocket borne measurements (kinetic energy ≈ 0.25 eV).

The beam is calibrated using a quadrupole mass spectrometer with a flow through ion source where beam particles can be analyzed directly, and an enclosed omegatron mass spectrometer where beam particles experience many wall collisions before ionization. The interpretation of the calibration data requires a knowledge of the velocity or the kinetic temperature of the beam particles and the ionization cross section ratios for atomic and molecular oxygen. The velocity distribution was not measured, but the experimental arrangement allows a reasonably firm determination of the kinetic temperature. The ionization cross sections have been taken from the literature. The application of the atomic beam system will be particularly useful for the calibration of quasiopen ion sources which are designed to minimize collisions of atoms with instrument surfaces before ionization. Atomic absorption and recombination, as well as the ion focusing characteristics of associated ion lens systems, can be evaluated. The beam system will be well suited for interaction studies of atomic oxygen with virgin surfaces which can be produced under ultrahigh vacuum conditions.

THE ATOMIC OXYGEN BEAM GENERATOR

Molecular oxygen is thermally dissociated on the surface of a heated tungsten filament. The method of thermal dissociation has been used very successfully for the dissociation of hydrogen molecules but only very little for the dissociation of molecular oxygen. Because of the strong chemical reactivity of oxygen and because of the high energy (5.09 eV) required for dissociation, not all metals which are successfully used for hydrogen dissociation are suited for oxygen dissociation. Large probabilities of dissociation are obtained only at temperatures above 2000 K. Only the refractory metals, tungsten, tantalum, and perhaps molybdenum can be brought to these temperatures without

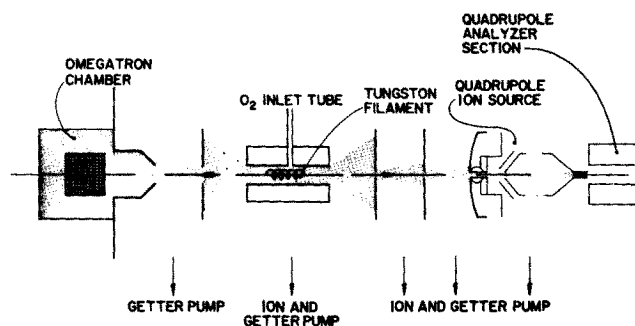


FIG. 1. Schematic diagram of the bidirectional atomic oxygen beam system.

melting or rapid evaporation. However, strong reactivity of these metals with oxygen leads to rapid formation of various oxides, resulting in both the destruction of the dissociating surface and the contamination of the atomic beam.

Experiments on the oxidation of tungsten carried out by Schissel and Trulson¹ showed that tungsten is a suitable metal for oxygen dissociation provided it is placed in a low pressure oxygen atmosphere ($<10^{-4}$ Torr) and kept at temperatures above 2200 K. At 2800 K nearly all of the impinging molecular oxygen is dissociated and reemitted as atomic oxygen. It remains to solve the geometric problem of exposing to oxygen only surfaces of sufficiently high temperatures, and to direct the emitted atoms so that a beam can be formed and its parameters can be quantitatively determined.

Most of the geometric problems are overcome by placing a hot tungsten surface (e.g., a filament) inside a tube which is made of nonreacting material. The tube is kept at a low temperature so that atomic recombination on the walls is low. Oxygen molecules injected at the center will then collide once or several times with the tungsten filament and the tube walls before they leave through the open ends. Multiple collisions of the molecules with the tungsten filament increase the net dissociation if the tube material is noncatalytic so that no significant wall recombination occurs. Tungsten oxides will also be formed because of repeated collisions of atoms with the tungsten surface. However, most tungsten oxide molecules condense on the cold walls of the envelope. With time, this condensation will change the surface properties of the envelope. The effect of such change on the atomic oxygen flux depends on the recombination and thermal accommodation properties of tungsten oxide.

TECHNIQUE FOR MEASUREMENTS OF THE FLUX INTENSITY AND THE RELATIVE CONCENTRATION OF ATOMS IN THE OXYGEN BEAM

Common atomic oxygen measuring techniques used in systems which operate at high pressure (0.1 Torr) are not

applicable here because of prohibitively low sensitivities. Mass spectrometers, similar to the units to be tested by means of the oxygen beam, have not been extensively used in laboratory experiments for atomic oxygen. However, experience gained in the present experiments has led to confidence in the use of mass spectrometers for flux calibration and composition determination. A combined use of a flow through ion source and an enclosed ion source mass spectrometer make it possible to obtain a flux calibration. The relative concentrations of atomic and molecular oxygen are determined with the flow through instrument, which is designed and placed so that only beam particles are detected. The absolute flux of molecular oxygen is then measured with an enclosed source instrument for which the sensitivity to molecular oxygen is quantitatively known. An omegatron system described by Niemann and Kennedy² was chosen as quantitative enclosed ion source detector of molecular oxygen and an Atlas quadrupole mass spectrometer type AMP 3, described by Brunee *et al.*³, was found to be suitable as a flow through source instrument. The ion source of the quadrupole had to be modified in order to use it for molecular beam detection. To avoid unpredictable mass and momentum discrimination among ionized beam particles in the source, it is necessary to direct the molecular beam parallel to the axis of the ion source and therefore terminate the beam in the instrument. Since the oxygen beam intercepted by the quadrupole ion source cannot be used simultaneously as a test beam for a target, a bidirectional oxygen beam source with symmetric particle flow is used. The principle is illustrated in Fig. 1. A narrow particle stream formed by apertures, enters the ionization region of the quadrupole ion source. The omegatron with the enclosed ionization region intercepts the beam on the target side. The orifice size determines the beam width. Intensive pumping in the source region and the space around the apertures is needed to minimize the background gas.

DETERMINATION OF THE FRACTIONAL DISSOCIATION AND THE RELATIVE CONCENTRATION OF ATOMS FROM QUADRUPOLE MEASUREMENTS

The number of ions produced in the ion source is proportional to the instantaneous particle density in the ionization region. To relate the measured density to the flux, it is necessary to know the average beam velocity or the kinetic temperature of the beam. The sensitivity of the quadrupole is a function of the ionization cross section of atoms or molecules, the electron beam current, the combined ion extraction efficiency of the source and the main analyzer section, the gain of the secondary electron multiplier, and the transfer function of the electrometer amplifier. All quantities except the ion extraction efficiency are constant

values for a particular species over a wide range of particle densities. The ion extraction efficiency may depend on the velocity of the particles, but in this particular experiment, where all particles are moving in the direction toward the analyzer, velocity discrimination is assumed to be negligible. For the detection of two different species, atomic and molecular oxygen, the ratio of the ionization cross sections, the differences in transmission efficiency of the quadrupole analyzer and quantum efficiency of the first dynode of the secondary electron multiplier must be known. The ratio of the ionization cross sections for atomic and molecular oxygen has been measured by Fite and Brackman.⁴ The difference in transmission efficiency has been evaluated for singly and doubly ionized argon atoms. Since the difference in transmission properties of the quadrupole between the mass 20 and 40 ratio and the mass 16 and 32 ratio is negligible, these measurements may be considered representative of the values for atomic and molecular oxygen. The difference in quantum efficiency of the first dynode of the secondary electron multiplier between masses 16 and 32 has not been directly measured, but from results of a study on an electron multiplier operated under similar conditions, and comparing direct current readings with pulse counting, the difference is believed to be negligible.

Knowing the sensitivities for atomic and molecular oxygen, it is possible to determine the degree of fractional dissociation, the fractional atomic oxygen flux and the relative oxygen loss due to absorption and oxidation by observing the peak heights of mass 16 and 32 when the dissociator is on and off. Because of the geometric arrangement of the oxygen source, the primary molecular oxygen flux into the source is constant and independent of the temperature of the tungsten surface. With the tungsten filament at room temperature, only molecular oxygen will be observed. When dissociation begins, the decrease in the molecular oxygen peak height will be proportional to the total amount of dissociation and oxidation.

The degree of oxygen conversion is given as

$$\bar{\gamma} = [\phi_c(O_2) - \phi_h(O_2)] / \phi_c(O_2), \quad (1)$$

where $\phi_c(O_2)$ and $\phi_h(O_2)$ are the molecular oxygen particle fluxes for no dissociation (cold tungsten) and dissociation (hot tungsten). Equation (1) can be expressed in terms of the kinetic temperatures of the beam particles $T_h(O_2)$ and $T_c(O_2)$ and the corresponding signal levels of the ion detector $U_h(O_2)$ and $U_c(O_2)$:

$$\bar{\gamma} = 1 - [T_h(O_2)/T_c(O_2)]^{1/2} U_h(O_2)/U_c(O_2). \quad (2)$$

The degree of conversion is an important quantity for the evaluation of the functioning of the atomic oxygen sources, but it does not determine the relative particle concentration in the beam since some of the dissociated oxygen reacts with the tungsten and forms an oxide. By

tuning the mass spectrometer to mass 16 the atomic oxygen flux is observed directly.

If $\phi_h(O)$ is the atomic oxygen flux then the effective fractional dissociation is

$$\gamma = \phi_h(O) / [\phi_h(O) + 2\phi_h(O_2)], \quad (3)$$

and the relative atomic flux is

$$\eta = \phi_h(O) / [\phi_h(O) + \phi_h(O_2)], \quad (4)$$

which, when expressed in terms of kinetic temperatures and signal levels of the current detector, become

$$\gamma = \left[1 + \left(2 \frac{T_h(O_2)}{T_h(O)} \right)^{1/2} \frac{\sigma(O)}{\sigma(O_2)} \frac{U_h(O_2)}{U_h(O)} \right]^{-1} \quad (5)$$

and

$$\eta = \left[1 + \left(\frac{1}{2} \frac{T_h(O_2)}{T_h(O)} \right)^{1/2} \frac{\sigma(O)}{\sigma(O_2)} \frac{U_h(O_2)}{U_h(O)} \right]^{-1}, \quad (6)$$

where $T_h(O)$ is the kinetic temperature of the atomic oxygen, $\sigma(O)/\sigma(O_2)$ is the ratio of the ionization cross sections of atomic and molecular oxygen, and $U_h(O)$ is the signal level of the atomic mass 16 measurement. The average ionization energy of the electron beam in the quadrupole ion source determined by a retarding potential analysis is found to be 75 eV. The corresponding ratio of the ionization cross section is $\sigma(O)/\sigma(O_2) | 75 \text{ eV} = 0.77$ (Fite and Brackman⁴). Provided the kinetic temperatures can be determined, the relative atomic concentration in the beam and the loss of oxygen due to oxide formation can be computed. It is noted that the mass 16 signal must be corrected for the contribution which results from doubly and dissociatively ionized molecular oxygen.

DETERMINATION OF THE ABSOLUTE PARTICLE FLUX

The absolute particle flux is measured on the target side of the beam source. A mass spectrometer is used with an ion source enclosed by a thermalization chamber. Beam particles which enter the orifice of the thermalization chamber collide many times with the walls of the chamber and the source electrodes before they enter the ionization region. Hence, it can be assumed that all particles are thermally accommodated and that the outgoing particle flux has an average velocity which is determined by the wall temperature. The particle density in the chamber is, therefore, proportional to the incoming flux but independent of the kinetic temperature of the particles in the beam. This is true provided that the pumping capacity of the vacuum system is large enough to prevent scattered beam particles from entering the chamber and particles which leave the chamber from reentering. If it is assumed that the conditions for adequate pumping can be satisfied and that the sensitivity of the closed ion source mass spectrometer can be determined by standard calibration

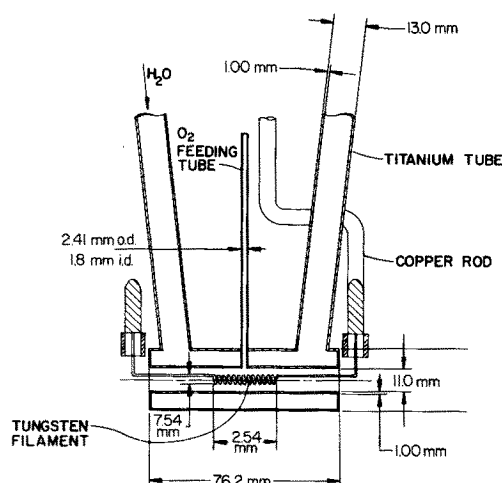


FIG. 2. Cross sectional view of the atomic oxygen source.

methods, the absolute flux into the orifice in the absence of dissociation will be given by

$$\phi_{\Omega c}(O_2) = \frac{1}{4} n_{\Omega}(O_2) \bar{v}_{\Omega}(O_2), \quad (7)$$

where

$$n_{\Omega c}(O_2) = U_{\Omega c}(O_2) / S_{\Omega}(O_2). \quad (8)$$

Here $\phi_{\Omega c}(O_2)$ is the molecular oxygen flux into and out of the chamber orifice, $n_{\Omega c}(O_2)$ is the instantaneous molecular oxygen density in the chamber, $\bar{v}_{\Omega}(O_2)$ is the average thermal velocity of the molecular oxygen in the chamber, and $U_{\Omega c}(O_2)$ and $S_{\Omega}(O_2)$ are the output signal level and the sensitivity of the mass spectrometer, respectively.

Because of the symmetry of the apparatus there is a one to one relationship between measurements of the quadrupole and the closed ion source instrument. A complete oxygen flux calibration can, therefore, be obtained.

There are, however, several possible sources of errors in this technique. The largest error is caused by the uncertainty in the temperature of the beam particles. Its effect on the measurement is discussed below. Errors also result from any uncertainty in the relative sensitivities of the quadrupole for atomic and molecular oxygen. Here the large contribution comes from the uncertainty in the ionization cross section ratio.⁵ The accuracy of the absolute flux measurement depends on the previous calibration with molecular oxygen and the repeatability of the instrument. The omegatron which was used for this experiment was calibrated with an error of $\pm 25\%$.⁶ The repeatability is better than $\pm 5\%$.² The error caused by the oxygen reaction on the hot filament is eliminated by the pressure calibration. It should be noted that absolute calibration errors can be reduced to at least $\pm 5\%$ by using standard pressure calibration techniques.

THE ATOMIC OXYGEN BEAM SOURCE

A cross sectional view of the source is shown in Fig. 2. A filament of high purity tungsten, commercially available from the R. D. Mathis Company, is placed in the center of a double walled titanium tube. Titanium was selected because of the low catalytic efficiency of its oxide.⁷ Cooling water flows between the tube walls to keep the surface at about 300 K while the tungsten filament is at 2800 K. The tungsten filament is supported at each tube end by heavy copper rods. These are extensions of high current ultrahigh vacuum feedthroughs which are mounted on a standard 7 cm Varian flange. The filament is heated with alternating current. Typical current and voltage levels for 2800 K filament temperatures are 75 A and 7.0 V. Molecular oxygen is fed through the narrow tube in the center of the double wall tube. The feeder tube is welded into the Varian flange on which the high current feedthroughs are mounted, and it is terminated with a Granville-Phillips variable leak. Molecular oxygen is supplied from a container via a two stage inlet system. A cold finger in the first stage of the inlet system is used for purification of the molecular oxygen. The assembled source is shown in Fig. 3. Oxygen which enters through the narrow feeding tube in the center will collide with the hot tungsten filament and escape at one of the ends of the titanium tube. The return

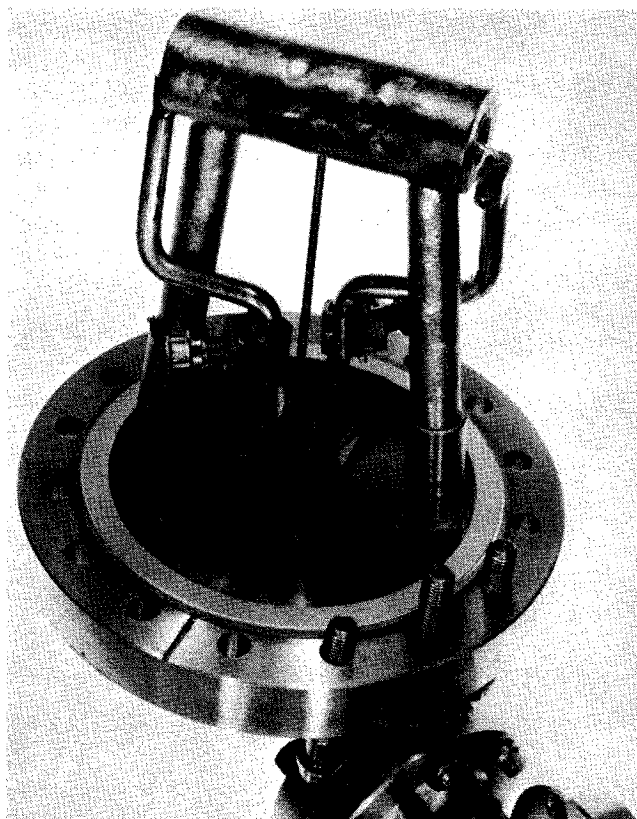


FIG. 3. Atomic oxygen source assembly.

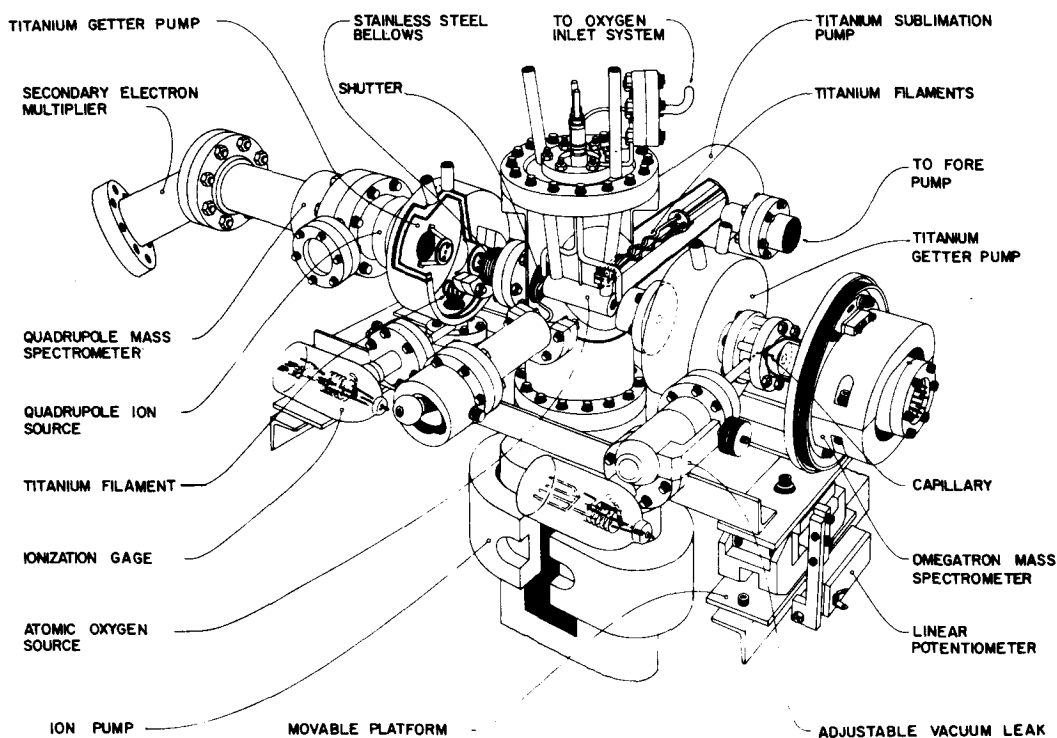


Fig. 4. Atomic oxygen beam system (complete assembly).

flux into the feeding tube is negligible because of the large difference between the inlet and exit tube diameter. Provided that the tungsten filament is kept at a high temperature (≥ 2800 K), and the molecular oxygen flux is kept below 10^{18} molecules $\text{cm}^{-2} \text{sec}^{-1}$, the oxide formation is small and most of the oxide formed condenses on the cold titanium walls.

THE VACUUM SYSTEM

In order to make the background pressure and the oxygen flux which does not directly originate in the oxygen beam source negligible, it is necessary to provide for fast gas pumping. The system should be free of hydrocarbons, and it should be bakeable at about 350°C .

The assembled system is shown in Fig. 4. A combination of a Varian 50 liter/sec sputter ion pump and a 400 liter/sec titanium sublimation pump is used as the main pumping system. The sublimation pump was modified so that the oxygen source could be placed directly in the main pump housing. Active titanium can then be deposited on the walls surrounding the source. Most of the oxygen emitted from the source strikes titanium activated surfaces directly, and the pumping speed is limited only by the sticking probability of oxygen on these activated walls. At room temperature the sticking probability of oxygen on continuously deposited titanium is approximately 0.6. It increases to near unity at liquid nitrogen temperatures.⁸

The quadrupole and the omegatron are mounted on the

sides of the main chamber and their ion source regions are connected to the oxygen beam source by collimating orifices and apertures. On the omegatron side the orifice diameter is 0.8 cm, and on the quadrupole side the aperture diameters are 0.1 cm. Liquid nitrogen cooled titanium getter pumps are used to maintain a low pressure in the spaces between the apertures. A double walled design was chosen to permit effective cooling of the pump surface by flowing liquid nitrogen through the space between the inner and the outer walls. Titanium is evaporated from a tungsten-titanium filament.

Bayard-Alpert type ionization gauges as shown in Fig. 4 are mounted on the getter pumps to permit a measurement of the background pressure in the pump space. It is expected that the gas particles in the pump will condense after the first or second collision with the cold walls, and thus provide a very low background flux for the omegatron and the quadrupole. This was confirmed in the experiment. Starting with a background pressure in the vacuum system of approximately 5×10^{-10} Torr a molecular oxygen flow was produced so that the measured molecular oxygen density in the omegatron corresponded to 2×10^{-6} Torr. At the same time, the pressure in the ionization gauge on the omegatron side rose to 7×10^{-10} Torr. By opening and closing a shutter which was placed in front of the source, the pressure in the omegatron chamber changed by approximately a factor of 500. Pressure measurements with the ionization gauge on the getter pump showed no pressure

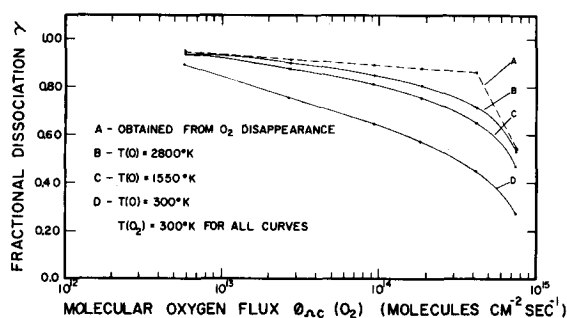


FIG. 5. Fractional dissociation versus molecular oxygen flux as measured at the omegatron orifice.

change. To provide for some pumping of noble gases, which can be introduced into the system as contaminants, a 20 liter/sec sputter ion pump is also connected to the ion source side of the quadrupole. For initial testing of the oxygen system, the omegatron with its getter pump was removed and a Pyrex window was mounted on the flange to allow direct optical inspection of the tungsten filament and the source chamber. After the initial heating of the filament for settling, a calibration was performed to relate the filament temperature to the applied alternating voltage and current. The temperature was measured with an optical pyrometer and temperature readings were obtained from the inside surface of the filament. No corrections were made for the transmission of the Pyrex window. At an operating temperature of 2800 K, the indicated temperature difference between the center and the end of the filament was about 100 K.

Since no optical inspection is possible when the omegatron and the quadrupole are mounted on the system, all quoted filament temperatures are obtained from the temperature-voltage calibration curve.

To condition the surface of the titanium tube and to decarbonize the tungsten filament, oxygen was admitted to the system until a pressure of approximately 1×10^{-6} Torr was reached. Then, the tungsten filament was heated to 2800 K for several hours, and it was expected that the titanium tube walls would be covered with several layers of titanium and tungsten oxide when the conditioning was terminated. Optical inspection of the tube walls showed a change in the surface color from a silver grey appearance to a milky grey color. No direct surface analysis was performed. Mass spectra which were taken with the quadrupole during this time showed argon, carbon monoxide, and methane in addition to oxygen.

BEAM STUDIES

After the initial preparation of the system, a number of atomic oxygen flux measurements were made over several decades of flux levels. A desired molecular oxygen level was set by means of the variable leak at the oxygen inlet

system. The absolute value was obtained from the omegatron reading. Data were recorded from both mass spectrometers for atomic and molecular oxygen. Then, the tungsten filament was heated to 2800 K and the decrease in the molecular oxygen was observed. After the flow stabilized, which required approximately 10 sec, a second sequence of mass 16 and 32 measurements was made. The tungsten filament was then cooled again and the initial flux measurement was repeated. During the measurements, the shutter was alternately opened and closed to avoid errors resulting from zero drift of the electrometer amplifiers. This sequence of measurements was repeated for several flux values, and the fractional dissociation was computed as outlined above.

The results are shown in Fig. 5. The fractional dissociation due to the hot tungsten filament surface is plotted versus the molecular oxygen flux measured at the omegatron when the tungsten filament is cold. The dashed line is the degree of dissociation computed from the disappearance of the molecules. The solid lines are the fractional dissociation computed according to Eq. (5). Curve B applies for an assumed atomic oxygen temperature of 2800 K; curve C was obtained by assuming as an example that the kinetic temperature of the atomic oxygen is equal to the arithmetic average of the filament temperature and the wall temperature of the surrounding tube. The wall

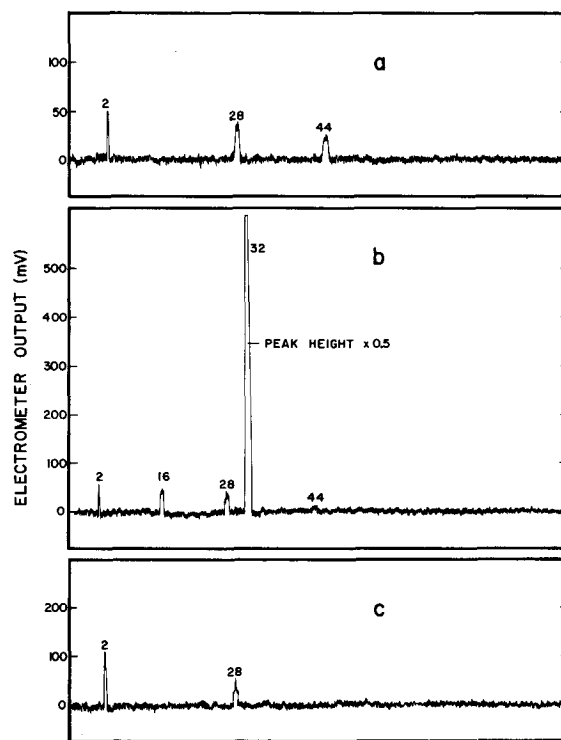


FIG. 6. Quadrupole mass spectra (tungsten filament at room temperature). (a) Background gases only. (b) With oxygen flux of 10^{14} molecules $\text{cm}^{-2} \text{sec}^{-1}$ at the omegatron orifice. (c) Same as (b) but shutter closed.

temperature is 300 K, so that the kinetic temperature is 1550 K. Curve D is computed by letting the kinetic temperature of the atomic oxygen be equal to the wall temperature of the titanium tube. In all cases, the kinetic temperature of the molecular oxygen is assumed to be 300 K.

As is seen from the curves of Fig. 5, an uncertainty is caused by the insufficient knowledge of the kinetic temperatures of the beam particles. Curves B and D represent the extreme cases.

The difference between the value obtained from the molecular oxygen disappearance and the atomic and molecular oxygen ion current ratios indicate a loss of oxygen with increasing flux. This is in accord with the theory which predicts an increase in relative oxide formation with increasing oxygen flux.

A typical set of quadrupole mass spectra taken with the tungsten filament at room temperature, thus, without dissociation, is shown in Figs. 6(a), 6(b), and 6(c). This is a control set of data for comparison with data under dissociative conditions. The first spectrum in the sequence [Fig. 6(a)] is the background spectrum. The second spectrum [Fig. 6(b)] was obtained when molecular oxygen was introduced into the system, and the third scan [Fig. 6(c)] was obtained with the shutter closed. It can be seen by comparing Figs. 6(a) and 6(c) that the background does not change when molecular oxygen is introduced. The small mass 16 peak in Fig. 6(b) is caused by doubly ionized and dissociatively ionized molecular oxygen. The ratio of the mass 16 to 32 peak heights is constant for a fixed set of quadrupole operating parameters. The apparent large variation in height of the hydrogen peak is a result of the statistical fluctuation of the signal. The width of the hydrogen peak is very small, allowing only a short time for measurement.

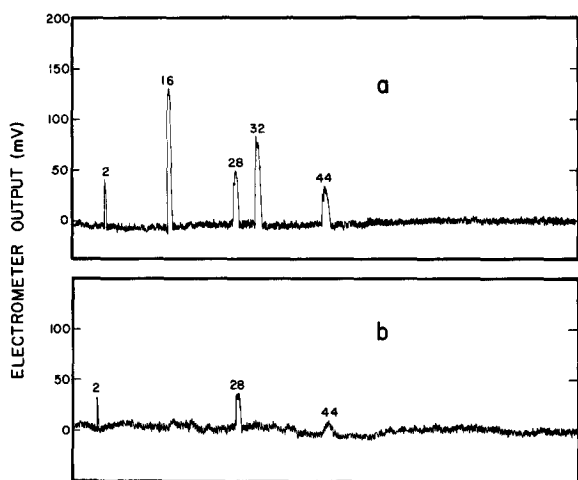


FIG. 7. Quadrupole mass spectra (tungsten filament at 2800 K) with a molecular oxygen flux of 10^{14} molecules $\text{cm}^{-2} \text{sec}^{-1}$ at the omegatron orifice. (a) Shutter open; (b) shutter closed.

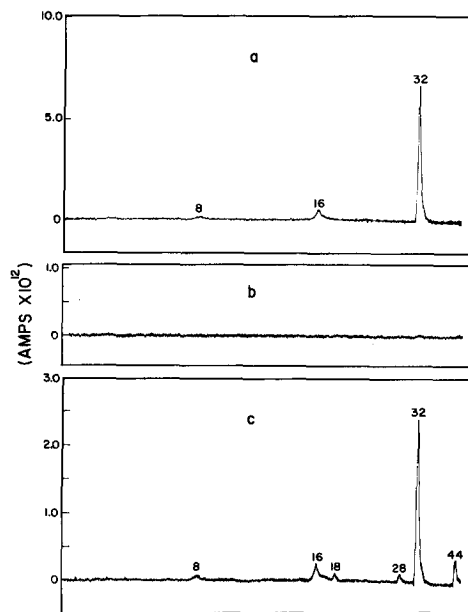


FIG. 8. Omegatron mass spectra, (tungsten filament at room temperature) with a molecular oxygen flux of $10^{14} \text{ cm}^{-2} \text{sec}^{-1}$. (a) Shutter open; (b) shutter closed; (c) tungsten filament temperature at 2800 K and shutter open.

A typical set of quadrupole mass spectra taken when the tungsten filament was heated to about 2800 K is shown in Fig. 7. The trace in Fig. 7(a) was obtained when the shutter was open and the trace in Fig. 7(b) when the shutter was closed. In comparing Figs. 6(b) and 7(a), the presence of a beam consisting primarily of atomic oxygen is clearly indicated in Fig. 7(a). The height of the atomic oxygen peak, when the filament is heated, is substantially lower than that of the molecular oxygen peak when the filament is cold, although the molecular oxygen leak rate was kept constant in the test sequence. This is due to the fact that the kinetic temperature of the oxygen atoms is expected to be near the temperature of the tungsten filament and the oxygen atoms move through the ionization region with a much higher speed than the oxygen molecules in the case when the tungsten filament is cold. Two offsetting factors are that the ionization cross section ratio of atomic to molecular oxygen for 75 eV electron energy is 0.77, and that each molecule produces two atoms. Again, in Fig. 6(c) as in Fig. 7(b) there is no evidence of a molecular or atomic oxygen background with the shutter closed. However, in Fig. 7(a) and Fig. 7(b), the mass 28 (CO) and 44 (CO_2) peaks are heightened as compared to the peak height of Fig. 6(a). By observing the time dependence of the peak heights it was concluded that these contaminants originate directly in the ion source region.

Finally, mass spectra were taken between atomic mass units of 160 and 250 in order to measure the tungsten oxide contamination in the oxygen beam. Even when the spectra were taken with decreased mass resolution and corre-

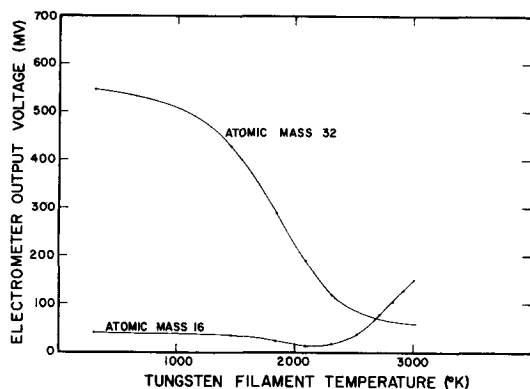


FIG. 9. Dependence of the mass 32 and mass 16 output signal on the temperature of the tungsten filament.

sponding increase in sensitivity, the amounts of tungsten oxide were below the detection limit of the quadrupole system.

A similar sequence of spectra was taken using the omegatron. Figure 8(a) corresponds to the quadrupole spectrum shown in Fig. 6(b) with the tungsten filament at room temperature. The effect of the shutter is demonstrated in Fig. 8(b). The last spectrum Fig. 8(c), which corresponds to the trace of Fig. 7(a) on the quadrupole side, was obtained when the filament was heated to 2800 K. Comparison of Fig. 8(a) and 8(c) with Fig. 6(b) and 7(a) shows that heating the tungsten filament has a considerably different effect on the omegatron measurement than on the quadrupole measurement. When the filament is heated, the peak height of the mass 32 peak in the omegatron decreases to approximately one-third of its height when the filament is cold, while the mass 32 peak height in the quadrupole measurement decreases to approximately one-tenth of its original height. Moreover, the ratio of the peak heights of mass 16 to mass 32 remains essentially unchanged in the omegatron, but a considerable increase in the ratio is noted in the quadrupole when the filament is heated. The fact that the ratio of the mass 16 and 32 peak heights remains unchanged indicates that essentially no atomic oxygen remains in atomic form in the omegatron chamber where ionization occurs. The mass 18, 28, and 44 peaks are water vapor, carbon monoxide, and carbon dioxide. These components are formed by surface reactions of atomic oxygen with hydrogen and carbon. The mass 16 and mass 8 peaks are caused by oxygen ions which are produced by dissociative and double ionization. Approximately 60% of the atomic oxygen which entered the chamber is absorbed on the surface and about 35% is recombined to molecular oxygen. With time the absorption decreased and the recombination increased. However, the test was terminated before saturation could be observed.

To test the dependence of the oxygen dissociation on filament temperature, a series of peak height measurements, using the quadrupole, was made for molecular and atomic oxygen for various values of filament temperatures. The results are shown in Fig. 9. The output voltages of the quadrupole electrometer are plotted versus filament temperature for a constant oxygen leak rate which corresponds to a flux of 8.4×10^{13} molecules $\text{cm}^{-2} \text{sec}^{-1}$ at the omegatron orifice. Above 1000 K the molecular oxygen signal decreases rapidly, reaching a plateau at about 2600 K. The mass 16 signal, which is the sum of the doubly ionized and dissociatively ionized molecular oxygen and atomic oxygen produced by the hot filament, decreases with increasing temperatures until a minimum is reached at about 2200 K. Above 2200 K atomic oxygen is emitted, and the signal increases rapidly, approaching a constant slope at the highest observed temperature. The mass 16 curve should reach a plateau at the temperature where 100% dissociation occurs. This plateau was not yet reached at 3000 K. It is noted, however, that the quoted temperature values are upper limits. The end sections of the tungsten filament are still at lower temperatures, and therefore a gradual increase in the effective dissociation can be expected.

In Fig. 10 are shown the degree of oxygen conversion (curve A) and the fractional dissociation for three assumed kinetic temperatures (curves B, C, and D). It can be seen that significant oxidation of the tungsten is occurring at temperatures below 1000 K, reaching a maximum value at about 2100 K. This is in general agreement with the results obtained by Schissel and Trulson.¹

The particular design of the quadrupole ion source required a narrow particle beam, if only direct streaming particles were to be ionized. Thus, only a narrow column of the oxygen beam can be analyzed at a given instant. In contrast, the omegatron orifice intercepts a much wider column, and the total flux into the orifice is an average value of the angular flux intensity. The particular geometry of the oxygen source does not suggest a uniform flux pattern.

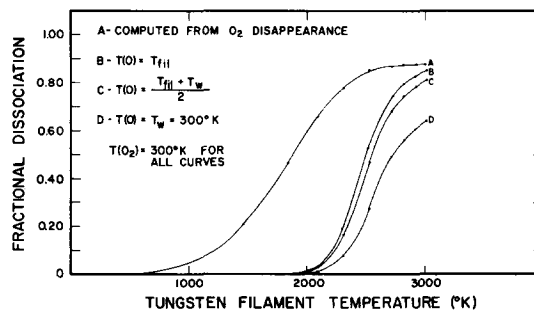


FIG. 10. Dependence of the fractional dissociation on the temperature of the tungsten filament.

To measure the flux pattern, the vacuum system was mounted on a moveable platform (Fig. 4), so that it could be either moved parallel or rotated relative to the target. A quasiangular scan is obtained by fixing the quadrupole to the reference frame and by moving the platform on the omegatron side. A true angular scan could not be obtained, because of the small separation of the source from the first aperture. Figure 11 shows the patterns obtained for molecular oxygen and atomic oxygen, respectively.

The curves show maxima when the quadrupole is so oriented that the intercepted flux originates from the titanium walls. The filament causes some obstruction in the center, and when the line of intersection moves toward the end of the titanium tube, the signal level decreases rapidly. In normal operation, the quadrupole is so oriented that the ion source intercepts a maximum flow. The operating point is marked on the curves.

DISCUSSION OF THE RESULTS

Two fundamental problems exist in the described method of generating atomic oxygen. These are the formation of undesirable tungsten oxides and the uncertainty in the flux calibrations.

The oxide content in the beam is largely reduced with the double wall tube design which allows most of the oxide to condense on the cold walls of the titanium tube. As long as the oxide buildup on the tube surface does not change the wall properties drastically, the problem is not critical. If, for example, the recombination efficiency on the walls is changed by the oxide, the atom to molecule ratio in the beam will change accordingly. But this ratio is measured during each test and difficulties arise only if the recombination probability approaches unity on the tungsten

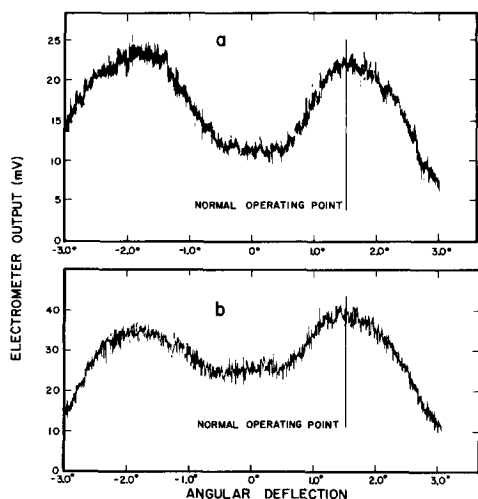


FIG. 11. Angular flux profile of the oxygen beam; tungsten filament at 2800 K. (a) Molecular oxygen; (b) atomic oxygen.

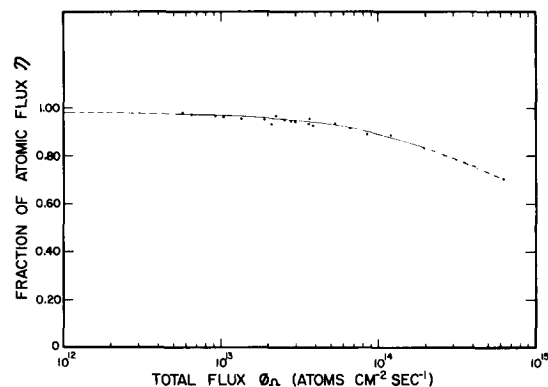


FIG. 12. Relative atomic oxygen flux versus total particle flux at the omegatron orifice, $T(O) = 2800$ K, $T(O_2) = 300$ K.

oxide. Finally, the thermal accommodation could be changed because of the tungsten oxide, and therefore the kinetic temperature of the oxygen would change. The resulting uncertainty in particle velocities relates to the second problem, flux calibration.

In the experimental arrangement, there was no direct way to determine the particle velocity. Thus, the possible values for the relative atomic oxygen concentration in the beam fall between curves B and D of Fig. 5. This uncertainty is reduced at low flux intensities where we can assume that nearly all primary molecular oxygen is dissociated. The situation is more complex at high flux levels where significant wall recombination may occur.

In all cases the oxygen atoms leave the tungsten surface with a velocity characteristic to the temperature of the tungsten filament. The geometry of the source permits some atoms to leave the source directly without any further collisions. Most of the atoms, however, will experience one or several collisions with the titanium walls and with the tungsten filament. If we assume that the atoms collide with the walls on the average 3.5 times (this is the numerical value of the collimation factor of the cylindrical source geometry) we can expect an effective accommodation of $a_{eff} = 1 - (1 - a)^{3.5}$ where a is the thermal accommodation coefficient after one collision. If a is 0.1,

$$a_{eff} = 1 - 0.9^{3.5} = 0.3.$$

If we assume that a_{eff} can be expressed in terms of temperature then

$$a_{eff} = (T_{fil} - T) / (T_{fil} - T_w),$$

where T_{fil} is the temperature of the filament, T_w is the wall temperature, and T is the kinetic temperature. We find the kinetic temperature to be approximately 2000 K when the tungsten filament temperature is 2800 K and the titanium wall temperature is 300 K. Since the average

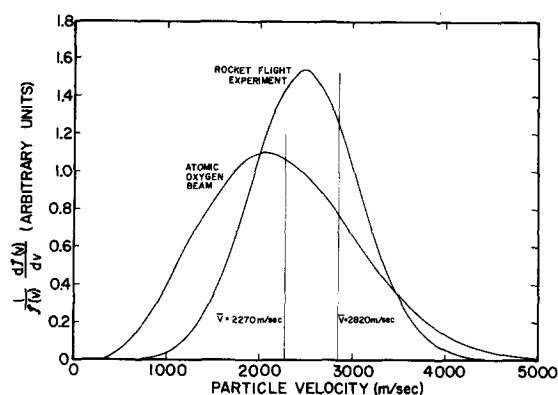


FIG. 13. Comparison of the atomic oxygen velocity distribution in the beam with the distribution encountered during a typical rocket flight at normal incidence.

velocity is proportional to the square root of the temperature, we find a change in the ratio of atomic to molecular oxygen by a factor of 1.18. This changes the values for the fractional dissociation only by 4% at the high flux level shown in Fig. 5. No data are available for the thermal accommodation coefficients on titanium oxide and tungsten oxide. Wise *et al.*,⁹ suggest a thermal accommodation coefficient for atomic oxygen on silicon oxide (SiO) of 0.01. One would expect a low accommodation coefficient for atomic oxygen from the following consideration. Atomic oxygen can stay on the surface for only a short time interval without either recombining with another atom or chemically reacting with the surface to form an oxide. Those atoms which do not recombine or react with the surface have spent little time on the surface (of the order of the period of the lattice vibration), in accord with the concept of small thermal accommodation.

Conditions are different for molecular oxygen. Molecular oxygen, which comes in contact with the hot tungsten surface and remains long enough to accommodate to that surface temperature, will dissociate. Only those oxygen molecules that do not collide with the tungsten filament or which do not thermally accommodate to the surface contribute to the molecular oxygen flux. The temperature of the fraction which results from atom recombination on the surface of the titanium tube is more difficult to predict, but this fraction should be small because of the low recombination coefficients of the titanium oxide and the small number of surface collisions of the atoms before emission from the tube. It can also be expected that the thermal accommodation coefficient for molecular oxygen on titanium oxide is significantly higher than for atomic oxygen. Wise *et al.*,⁹ measured a value of 0.17 on SiO. Since the velocity distribution has not yet been measured directly, it is assumed that the atomic oxygen is emitted with a kinetic temperature equal to the temperature of the tungsten filament and the kinetic temperature of the

emitted molecular oxygen is equal to the wall temperature of the titanium tube. The relative atomic flux in the beam was computed for several total flux values for a filament temperature of 2800 K and a wall temperature of 300 K. The results, illustrated in Fig. 12, show that the beam consists of more than 80% atomic oxygen at flux levels of 2×10^{14} atoms $\text{cm}^{-2} \text{sec}^{-1}$ at the target distance.

Inspection of Fig. 5 shows that the value of the fractional dissociation computed from the mass 16 to 32 ion current ratios decreases more rapidly with incoming flux than the values for the molecular oxygen conversion. This indicates a loss of oxygen which can result either from permanent absorption on the surface of the titanium oxide walls or from oxidation of the tungsten filament. If the oxygen disappears because of absorption on the titanium oxide walls, one would expect the absorption to be more effective at low flux levels where saturation does not occur rapidly. However, the trend is just the opposite. Moreover, saturation, or at least a reduction in absorption, should occur after several hours of operation. This was not observed.

A comparison of these data with computed oxidation rates using the rate constants and oxidation processes published by Schissel and Trulson¹ was made. Agreement was obtained if the difference between the O_2 disappearance and the mass 16 and 32 ion current ratio is attributed to loss of oxygen due to oxide formation at the tungsten filament.

In Fig. 13 a comparison is shown of the assumed velocity distribution of the oxygen atoms in the beam with the distribution encountered in a rocket experiment. The kinetic temperature of the atomic oxygen in the beam is assumed to be 2800 K. The rocket velocity is chosen to be 2000 m/sec and the temperature of the ambient atomic oxygen in the atmosphere at about 200 km is chosen to be 750 K. The curves shown in Fig. 13 are normalized so that they enclose equal areas; the average velocities are 2270 m/sec for the thermal beam and 2820 m/sec for the rocket experiment.

ACKNOWLEDGMENTS

I am indebted to Professor William G. Dow for many stimulating discussions and suggestions and for his continuous encouragement of this work. I wish to thank Mr. George R. Carignan for valuable advice and for making available the facilities of the Space Physics Research Laboratory. I am also indebted to Mr. Nelson W. Spencer for his interest in the experiment and his helpful criticism. The invaluable assistance of Mr. Frank S. Lee throughout the experimental phase of this work and the help of Mr. Bud G. Campbell in the preparation of drawings and figures are gratefully acknowledged.

* The research was supported by the National Aeronautics and Space Administration, Contract No. NAS5-9113, Goddard Space Flight Center, Greenbelt, Md. 20771.

† Present Address, Code 623, Laboratory for Planetary Atmospheres, Goddard Space Flight Center, Greenbelt, Md. 20771.

¹ P. O. Schissel and O. C. Trulson, *J. Chem. Phys.* **43**, 737 (1965).
² Hasso B. Niemann and Brian C. Kennedy, *Rev. Sci. Instrum.* **37**, 722 (1966).

³ C. Bruneel, L. Delgmann, and K. Kronenberger, "The Atlas Quadrupole Mass Spectrometer," paper presented at Mass Spectrometry Conference, ASTM Committee E-14, San Francisco, (1963). Published by Atlas Mess-und-Analysen Technik, GmbH, Bremen, Germany.

⁴ W. L. Fite, and R. T. Brackmann, *Phys. Rev.* **113**, 815 (1959).

⁵ L. J. Kieffer and Gordon H. Dunn, *Rev. Mod. Phys.* **38**, 1 (1966).

⁶ N. W. Spencer, L. H. Brace, H. B. Niemann, G. R. Carignan, and D. R. Taesch, 6th Intern. Space Sci. Symp. Space Res. **VI** (1965).

⁷ J. E. Morgan and H. I. Schiff, McGill University, Montreal, Province of Quebec, Canada, (1965), Tech. Rep. Contract No. AF19(628)-2425.

⁸ R. E. Clausen 1961 Trans. 8th Natl. Vac. Symp. (Amer. Vac. Soc.) Combined with the 2nd Intern. Cong. Vac. Sci. Technol. (Intern. Org. Vac. Sci. Technol.) **1**, 345 (1962).

⁹ H. Wise, B. J. Wood and Y. Rajapakse, *Phys. Fluids* **9**, 1321 (1966).

Electronic Linearization of Temperature Using a Dual Element Sensing Technique

JOHN MASSEY

Massey Engineering Company, 202 N. Highland Street, Arlington, Virginia 22201

(Received 26 January 1972; and in final form, 17 February 1972)

All known temperature sensors today have some degree of nonlinearity. An analytic technique using a dual element sensing probe with a bridge type electrical thermometer is developed to reduce the magnitude of deviation from linearity. Specific algebraic solutions for nickel (concave upward) and platinum (concave downward) transducer materials are generated using this dual element technique, showing a significant improvement in linearity; i.e., worst case tracking errors are reduced to ± 0.25 and ± 0.043 °C for nickel and platinum, respectively, over the range -40 – 260 °C. Instrumentation of this technique for practical applications is discussed, leading to the development of a portable direct reading electronic thermometer having a worst case total error of 0.01 °C per year over the 0–100 °C range.

INTRODUCTION

As early as 1916, metrologists¹ have been working on techniques to linearize an output variable as a function of temperature. Utilizing the resistance or conductance characteristics of materials as the output variable, experimenters have found that the nonlinear temperature resistance characteristics (R_T) of all known stable elements fall into four categories² as illustrated by the R_t vs t curves in Fig. 1. Typical examples of each type are given with nickel (curve A) and platinum (curve C) providing a wide variation of thermometry features notable for further discussion. With the nonlinearity characteristics of each transducer material known, a calibration table for each type of material in various thermometer configurations can be generated. To date, techniques for temperature measurement require, in addition to the physical sensor measurement, (i) a manual reference to a sensor table and (ii) an extrapolation for values between recorded data points, to account for the degree of nonlinearity, a cumbersome and time-consuming method at best. It is the main objective of this paper to develop and illustrate a patented³ method of linearizing temperature measurement electronically, reading out direct values in real time, without lengthy calculation, with a substantially higher degree of accuracy and reliability than present systems provide.

PRESENT LINEARIZATION TECHNIQUES

The work of many linearization researchers has been summarized very clearly by Diamond.² Linearization can be divided into four classes: (a) null balance bridges with sensing devices to provide a constant rate of change of slope of the set point resistance¹⁻⁸; (b) function generator techniques which use passive devices to generate the resistance vs temperature curve of some material⁹⁻¹¹; (c) deflection methods which are non-nulled bridges which combine the curve of the output current of a bridge with the curve of a sensing element (plus, on occasion, curves of other variables) to provide a constant output slope¹²⁻¹⁹; (d) nonlinear dial displays which set the spacing of the dial to give correct readout.²⁰

Combining method (a) a null balance bridge, with a dual element sensor technique will be shown to provide vast improvements in linear deviation, e.g., from 28 to 0.25 °C for nickel in the range -40 – 260 °C.

Although dual element linearization is in its infancy, it should be noted that any of the present techniques will provide a degree of linearization sufficient for some requirements and needs. In general, though, any good linearization method should (a) provide some minimum required worst case tracking error, depending on the application; (b) be physically realizable, i.e., economical, maintainable, usable